Pacific Atmospheric Sulfur Experiment

Project Description

1 Introduction

Pacific Atmospheric Sulfur Experiment (PASE) is a comprehensive study of the chemistry of sulfur in the remote marine troposphere. A major part of PASE will be devoted to the chemistry and physics (primarily of sulfur) in a cloud free convective boundary layer (CBL). Our strategy is to first understand the chemistry and physics of gases and aerosols (including cloud condensation nuclei, CCN) in a cloud free environment before trying to understand systems containing cloud. Studies of systems containing cloud can be logically built on an understanding of cloud free systems. PASE also will focus on developing a better understanding of the buffer layer (BuL) and formation of new particles in the cloud outflow of marine cumulus.

PASE will provide information on aerosol chemistry and physics in the remote marine atmosphere essential for developing an understanding for the Aerosol Indirect Effect (AIE) in this region. However, as alluded to above, PASE is just a first step in this process. PASE will also explore key elements of the CLAW (Charlson, Lovelock, Andreae, Watson [1987]) hypothesis that describes how dimethyl sulfide oxidation can have important impacts on AIE. At the core of PASE is the chemistry of sulfur because much of the chemistry of AIE in the marine atmosphere involves the products of dimethyl sulfide (DMS) oxidation and their interactions with aerosols. The detailed information on sulfur chemistry of both aerosols and gases obtained in PASE will make a major contribution to understanding the link between sulfur chemistry and the evolution, growth, and properties of aerosols in the marine atmosphere. We expect that our measurements will allow us to test the viability of the atmospheric sulfur portions of the CLAW hypothesis even if they cannot fully resolve the issue.

Much of PASE will be conducted in the CBL of the marine atmosphere east of Christmas Island (Kiritimati) during a cloud free period in August 2007. This CBL is exceptionally well mixed. Its turbulence and wind fields have very small vertical and temporal variability and the very high solar intensity is ideal for driving photochemistry. The high and spatially uniform DMS flux is another important characteristic.

PASE also will revisit new particle formation in cloud outflow and will include the influence of processes in the buffer layer. Sufficient cloud should be present especially during unstable periods which occur every few days. If not, then flights north toward the intertropical convergence zone (ITCZ) should intercept sufficient cloud for the experiment. A mission meteorologist (Merrill) will be onsite with phone, internet and fax communications to help plan these flights throughout PASE.

State of the art instruments will be used to make accurate and high speed airborne determinations of sulfur dioxide (SO_2), dimethyl sulfide, dimethyl sulfoxide (DMSO, dimethyl sulfone ($DMSO_2$), methane sulfonic acid (MSA), sulfuric acid (H_2SO_4), hydroxyl radical (OH), peroxyl radical (HO_2), ammonia (NH_3), water vapor (H_2O), ozone (O_3), hydrogen peroxide (H_2O_2), methyl hydrogen peroxide (CH_3OOH), liquid water, temperature, pressure, wind velocity. DMS, SO_2, H_2O and O_3 will be determined at 25 samples per second allowing vertical fluxes of these species to be determined by eddy correlation. Chemical budgets for the sulfur species can be calculated from the concentrations and fluxes. These budgets will contain valuable information on chemistry in general but specifically on their chemical formation and destruction rates.

The entire suite of NCAR aerosol probes available for C-130 will be flown. In addition, PI's will measure size and volatility (0.15-10.0 um), size and volatility (0.01-0.3 um), size resolved mixing state, refractory and volatile number, ultrafine number concentration, absorption coefficient (Black Carbon), whitecap/bubble coverage, size integrated ambient total ions around a circle, leg average size resolved ions, coarse particle size distribution, fast submicron aerosol ion composition, CCN concentration and supersaturation spectrum. Aerosol non-sea salt sulfate (NSS), methane sulfonate (MS), sodium, ammonium, calcium, magnesium, nitrate, oxalate, chloride, bromide and organic carbon will be determined using filter and impactor methods, integrated over 30 minute constant-altitude legs.

As stressed above most of PASE is a study of the chemistry and physics of a cloud free marine CBL.

From time series obtained in 9 hour nighttime and daytime flights in a well mixed cloud free convective boundary layer, the time evolution of gases, aerosols (including composition as a function of size), and CCN in a system free of liquid water will be obtained perhaps for the first time. PASE data will provide restraints for models of aerosols, gases and CCN in dry systems that are necessary for understanding and modeling systems containing liquid water. Ten flights of PASE will be conducted in a Lagrangian framework similar to that used in the Dynamics and Chemistry of Marine Stratocumulus Study (DYCOMS) I and II programs. The Lagrangian framework allows the budgets of dynamical properties, H_2O, O_3, DMS, and SO_2 to be determined experimentally with few approximations.

Using entrainment models for transport across the CBL top, flux estimates will be derived for aerosols and gases which are not determined fast enough for the fluxes at the CBL top to be obtained by the eddy correlation technique. Faloona et al. [2005] showed that in DYCOMS II, fluxes of DMS, O_3, and H_2O at the CBL top and concentration jumps across the CBL top could be used to compute entrainment velocities with which the fluxes of species measured at slower rates could be determined. Examples of gases in this category of more slowly measured species are DMSO, $DMSO_2$, H_2O_2, NH_3, MSA, H_2SO_4 and CH_3OOH.

Modeling of the chemistry and dynamics of the marine trade wind regime is an integral part of PASE. Issues such as the photochemical formation of small particles of sulfuric acid in the outflow of cumulus cloud will be investigated and evaluated for their potential to grow to CCN by accreting gases such as, H_2O, SO_2, NH_3, MSA, and H_2SO_4.

The use of entrainment velocities and measured concentration jumps across the CBL top also can be used to compute the fluxes of CCN and aerosol at the CBL top. The fluxes of CCN and aerosol at the CBL top allow models of the source of aerosol and CCN to be tested. Since the formation of new particles in the CBL is rarely observed there must be other sources. One hypothesis advanced by Raes [1995] is that the new particles are formed in the free troposphere, particularly in cloud outflow [Perry and Hobbs, 1996; Clarke et al., 1997], and are later brought into the trade wind system and then to the CBL where they grow into larger particles by accreting H_2O and H_2SO_4. The underlying hypothesis is that these sulfur containing particles are or will become CCN.

The origin of small particles and their growth to larger particles and CCN are core issues in developing an understanding of AIE and in testing CLAW. Another intriguing hypothesis that can also be tested is that small particles, formed by wave breaking, grow by accreting H_2O and H_2SO_4 and that these particles with a sea salt core are also CCN. The formation of nanometer size sea salt preCCN will be studied including their potential growth to CCN. Loss of SO_2 and H_2SO_4 to aerosol surface area, including sea salt near the ocean surface, will be intensively studied. Using some assumptions, fluxes of CCN and aerosol at the ocean surfaces can be estimated.

Finally, the research described can be perceived as part of a longer term effort of atmospheric scientists to understand the chemistry and physics of the marine atmosphere. A representative specific goal of this perceived long term effort is to develop accurate mathematical representations of the aerosol indirect effect (AIE) in marine cloud which is a major cooling term in Earth's radiation budget. A specific goal of this proposal is to test the viability of the chemistry and aerosol physics which underlie the CLAW hypothesis. As mentioned above PASE is a first step in developing an understanding of AIE and in testing CLAW since it is done in a simplifying cloud free CBL.

The marine atmosphere, however, is an exceedingly complex place. So much so in fact, reliable models of AIE and quantitative tests of CLAW have so far eluded atmospheric scientists. Although difficult, these issues are sufficiently important to justify the long term goals of understanding and quantifying AIE and testing CLAW.

2 Research

Substantial progress has been made during the last 30 years in understanding the chemistry of atmospheric DMS. This progress was recently summarized by Davis et al. [1999] and extended by Chen et al. [2000]. That DMS was the major sulfur gas emitted to the atmosphere was shown through determinations of DMS in marine air by Lovelock [1972] and Maroulis and Bandy [1977] and in seawater by Andreae

and Raemdonck [1983]. Given that source, it was not surprising that aerosols in pristine marine air contained substantial levels of non-sea salt sulfate and methane sulfonate [Savoie and Prospero, 1989] as products of DMS oxidation. Laboratory studies have shown that DMS oxidation can be initiated by OH, by halogen containing radicals, and by the NO_3 radical [Davis et al., 1999]. In the clean atmosphere around Christmas Island, OH appeared to be the most important DMS oxidant starting reactions that lead to SO_2, H_2SO_4, DMSO, $DMSO_2$, MSA, MS [Davis et al., 1999], and NSS aerosol. Although the basic chemical framework seems clear, many unknowns remain. In this section, we outline specific areas that will be addressed.

2.1 Fast measurements and chemical budgets

Instrumentation is now available for determining DMS and SO_2 at 25 samples per second (sps) aboard ships and aircraft making possible the use of eddy correlation for determining surface and entrainment fluxes. Atmospheric sulfur chemistry has not been tested using direct measurements of DMS source- and SO_2 loss-fluxes as described in this proposal. Methods also are available for at least 1 sps determinations of DMSO and $DMSO_2$ [Nowak et al., 2001; Xu, 1999], thus allowing these species to be profiled. It may even be possible to make 25 sps determinations of DMSO and $DMSO_2$ so their fluxes could be computed by eddy correlation.

2.2 DMS and SO_2 Chemistry

A major goal of the proposed research is to experimentally determine all the terms in the chemical budgets of DMS and SO_2. The budgets of DMS and SO_2 contain the surface fluxes of these species, the oxidative destruction of DMS and the gas phase formation and destruction rates of SO_2; the quantities needed to test kinetic models of their chemistry.

Complete budgets for these species have not been obtained although some attempts have been made. Davis et al. [1999] and Chen et al. [2000] summarized these attempts. All reported budgets are incomplete because the necessary fluxes at the boundary layer top and bottom for DMS, SO_2 and other species were not available. Consequently, fluxes were parameterized and thus contained adjustable variables that were selected by best fit to the available data. A major contribution of the proposed study is that DMS and SO_2 budgets will be closed using directly determined eddy fluxes at the ocean surface and interfacial layers.

2.2.1 DMSO and $DMSO_2$ Chemistry

Models of DMS oxidation chemistry include an OH-addition channel that produces MSA, DMSO and $DMSO_2$ [Davis et al., 1998]. Since the efficiency of this channel apparently increases as temperature decreases, DMSO and $DMSO_2$ concentrations should increase when the ambient temperature drops. The Christmas Island site has air and ocean temperatures on the high side, near 26°C, which should make this channel relatively inefficient compared to ocean areas having lower temperatures. Photochemical production should cause MSA, DMSO and $DMSO_2$ to increase during the daytime, while at night they should decrease due to uptake by aerosol surfaces and the ocean.

However, observations of DMSO and $DMSO_2$ on Christmas Island in 1994 showed no diurnal variation [Bandy et al., 1996]. This is in contrast to the obvious anticorrelation of DMS and SO_2 observed by Bandy et al. [1996]. More recently Nowak et al. [2001] found a similar lack of an identifiable diurnal variation for DMSO and $DMSO_2$. Clearly, these data do not match model predictions, so something has been missed. As Nowak et al. [2001] point out, either the kinetic models are wrong or a non-photochemical source of DMSO has been missed. An objective of this program is to make more accurate measurements of DMSO, $DMSO_2$, and related species over time and altitude, to resolve this issue.

2.2.2 BrO and DMS Chemistry

Because appropriate instrumentation is not available to study bromine chemistry in detail we must consider our efforts to be exploratory in nature. However, review of the literature suggests that the issue remains and must be considered.

von Glasow et al. [2002a, 2002b, 2004] numerically modeled the impact of gas and droplet halogen chemistry on photochemistry (in particular for DMS oxidation) in both clear and cloudy marine boundary layers (MBL). In these studies the inclusion of a bromine oxide (BrO)-DMS oxidation path contributed approximately 17% to 75% of the total DMS oxidation under equatorial Pacific (remote marine tropical) to "Cape Grim summer" conditions. This model predicts that the BrO-DMS path yields DMSO and has a significant impact on the DMSO to DMS ratio. Under the low nitrogen oxide conditions of the equatorial tropics, the other DMS oxidant is OH. Ozone is the key constituent regulating the relative importance of the BrO mechanism [von Glasow et al., 2004] as was also shown for ozone production [Chang et al., 2004]. Ozone chemistry effectively controls both the BrO source and the OH source. Further, the addition of BrO chemistry was shown to reduce the efficiency of DMS to SO_2 conversion in the gas phase and the inclusion of heterogeneous halogen chemistry increased the production rate of MSA and non-sea salt sulfate. In clear air aerosol simulations, halogens contributed roughly 50% of the NSS production; in cloudy air simulations H_2O_2 accounted for more than 90% of NSS production. The reductions noted in SO_2 also reduced gas phase H_2SO_4 production and reduced "nucleation" of new particles. BrO levels of consequence to DMS are estimated to be on the order 0.3-3 ppt.

The contribution of BrO and halogen chemistry to DMS oxidation in our study region is expected to be small. BrO chemistry is associated with the loss of Br^- from sea salt aerosols. Evidence of Br^- loss, e.g. Br/Na ratios below that of seawater, and that of other halogens, e.g., F, would indicate the potential presence of halogen chemistry. Some PI's will address this issue in more detail in their proposals.

2.3 Loss of SO_2 to the sea salt aerosol layer

The absorption of SO_2 and its oxidation to SO_4^{-2} by O_3 in water contained in sea salt particles is widely accepted as a major pathway for the removal of SO_2 from the MBL. The newly formed sulfuric acid might then displace hydrochloric acid (HCl) and other chlorinated gases from these concentrated solutions. Martens et al. [1973] reported the depletion of chloride in Puerto Rican and San Francisco Bay marine aerosol, while Gravenhorst [1978] reported that SO_2 was lost to marine aerosols of the North Atlantic. A transect from 30°N to 30°S in the Central Pacific also revealed that this loss was pronounced in the upwelling region of the equatorial Pacific near Christmas Island [Clarke et al., 1997].

Numerous reports of non-sea salt sulfate (NSS) enrichment and chloride depletion followed this initial work. The papers of Keene et al. [1990], Chameides and Stelson [1992], Suhre et al. [1995], Luria and Sievering [1991] are typical. These studies postulate the existence of suitable mechanisms for the oxidation of SO_2 by O_3 in marine aerosol, in agreement with field studies showing NSS enhancement and chloride (Cl^-) depletion. All predict that SO_2 removal by marine sea salt aerosol is at least as efficient as removal at the sea surface. However, until now, removal of SO_2 at the sea surface could not be directly observed. An important objective of this work is to determine the nighttime budgets of SO_2 with high precision below 200 m. In the cloud-free case at night the destruction term for SO_2 above the ocean surface is only loss to aerosol because the photochemical loss is nil. The surface flux can be obtained by extrapolating the vertical SO_2 flux in the CBL to the ocean surface

2.4 Aerosol and CCN evolution

PASE is designed to obtain the temporal evolution of the aerosol size distribution and CCN saturation spectra corrected for entrainment from the buffer layer and for loss to the ocean. Fluxes of relevant species at the CBL top will be obtained from entrainment models using measured jumps at the CBL top and entrainment velocities obtained from the fast H_2O, SO_2, DMS and O_3 data. Using this approach the daytime increase in NSS, MS, and possibly other specie concentrations can be corrected for entrainment. Surface loss is probably small because the particles are quite large and diffusion rates to surfaces very slow. However, corrections for surface loss will be made using appropriate models (described by Clarke and Huebert in their proposals).

Although not done previously it is believed that the aerosol distribution and CCN saturation spectra can divided into bins and particles and CCN of appropriate size and supersaturation respectively added to the bin from entrainment are removed and aerosol and CCN lost to the ocean are added (because of their

mass loss of CCN and aerosol to the ocean surface should be slow). The result is a distribution of size for aerosol and supersaturation that represents only processes in the CBL. The evolution of aerosol size and CCN supersaturation spectra corrected for entrainment and loss to ocean surface will be followed during the 9 hour flights and will reflect processes driving the evolution of the size distribution and CCN saturation spectra whatever that may be. Current wisdom is that at night, when DMS oxidation is not the driving force, aerosol sinks and CCN sinks may be the driving process whereas in daytime DMS photooxidation is the main driving force. Regardless of whether or not current wisdom prevails, these data will be a severe test of models of the chemistry and physics of the cloud free marine CBL.

2.5 Cloud Processes and New Particle Production

Clouds form upon cloud condensation nuclei that have the size and chemical properties allowing them to activate at prevailing cloud supersaturations. The increased surface area of the activated droplets can enhance the rate of gas to particle conversion and promote aqueous phase reactions that can increase net solute mass as a result of non-precipitating cloud cycles. This growth process can provide a sink for gas phase SO_2 and also result in a so-called Hoppel minimum in the size distribution between unactivated and activated sizes [Hoppel and Frick, 1994]. The diameter of this minimum provides an indication of representative cloud supersaturations for the region [Cantrell et al., 1999]. Ground based measurements of diurnal variations in this minimum at Christmas Island were interpreted to reflect photochemical production and cloud processing [Clarke et al., 1996]. Recently, airborne studies near tropical clouds have been argued to demonstrate the effectiveness of this process [Jimenez et al., 2004] although the instruments were not ideal for this purpose and uncertainties were large. We will explore this process in greater detail with the far more complete and faster measurements available during PASE. These flights will require measurements below, in, above and around non-precipitating clouds to examine changes in the size distributions and chemistry. Stratification of observed changes in terms of cloud air sources identified by conservative variables (e.g. DMS and equivalent potential temperature) will be employed [Paluch, 1979].

Cloud outflow regions have also been shown to be a source region for new aerosol particles [Clarke et al., 1998] and often consistent with binary nucleation of sulfuric acid [Clarke et al., 1999]. These near cloud environments were found generally well above 2 km in the tropics although in highly productive regions after heavy rain we found evidence of boundary layer nucleation [Clarke et al., 1998] linked directly to the sulfur cycle. We will revisit the formation of new particles in the outflow region of marine cumulus clouds. Our fast OH, DMS, SO_2, DMSO, H_2SO_4, H_2O, NH_3, aerosol composition and liquid water instruments replace very slow instruments which could not resolve the outflow regions observed in earlier experiments. PASE will have a greatly improved capability to make progress on this problem. The studies will be carried out as they were in ACE-1 where the favorable clouds were first detected by satellite observations but the study clouds were located after the experiment was airborne. The mission meteorologist (Merrill) will be onsite with internet, phone and fax communications to perform these planning activities. If necessary, flights may be made north toward the ITCZ to encounter suitable cloud formations.

2.6 Peroxides

Hydrogen peroxide concentrations, and to a lesser extent CH_3OOH concentrations, in the marine boundary layer are impacted by physical processes as well as photochemical production and loss [Thompson and Cicerone, 1982 Thompson et al., 1993; Heikes et al., 1996; Chen et al., 2001; Chang et al., 2004]. Surface deposition and entrainment fluxes of several chemical constituents (DMS, SO_2, H_2O and O_3) will be determined in PASE using 10 Hz or faster instrumentation and correlative Reynolds flux methods. The entrainment velocities developed from the correlative methods will be combined with slower measurement gradient flux methods to evaluate entrainment fluxes for H_2O_2 and CH_3OOH between the free-troposphere, the buffer layer and the marine CBL as described by Lenschow et al (1999). Chang [2002] and Chang et al. [2004] theoretically showed that the entrainment of H_2O_2, CH_3OOH, and formaldehyde (CH_2O) played a minor role compared to photochemistry in setting the mixing ratio of these species in the MBL. However, the entrainment of O_3, nitrogen oxides, or hydrocarbons was shown to impact their own mixing ratio, as well as, those for H_2O_2, CH_3OOH, and CH_2O via photochemistry. PASE permits a venue to evaluate their

theoretical results.

2.7 Dependence of SO_2 exchange velocities on wind speed

Surface fluxes of gases are thought to be the product of an interfacial concentration difference and an exchange velocity. This exchange velocity (which can be generalized to many gases) is thought to be a function of surface wind speed [Liss and Merlivat, 1986; Wanninkhof and McGillis, 1999], surface films, whitecaps, and other factors. Recent measurements of CO_2 fluxes suggest that other water-side controlled gases like SO_2 might show a cubic dependence on wind speed [Wanninkhof and McGillis, 1999], although a quadratic has often been used [Wanninkhof, 1992]. We propose to examine these relationships using direct surface flux measurements of SO_2 obtained using eddy correlation. The negligible concentration of SO_2 in the surface ocean obviates the needs for seawater measurement.

2.8 Photochemical Models

Photochemical modeling will be performed by Yuhang Wang at Georgia Tech through a contract from Drexel University. Dr. Doug Davis will be a co-investigator. A photochemical model will be developed based on a model reported by Davis et al. [1999] that was used to study the chemistry of sulfur in the tropical marine atmosphere including the Christmas Island trade wind regime. This model will be will be modified to reflect knowledge gained about the chemistry, sources and sinks of species such as DMSO and $DMSO_2$.

3 Proposed Research

The important objective of this work is to uniquely obtain chemical budgets. The approach for doing this was developed by Bandy and Lenschow [Lenschow et al., 1988] for the DYCOMS I program that was further refined in the DYCOMS II program [Faloona, et al., 2005; Stevens, 2003]. Fast determinations of DMS, SO_2, O_3 and H_2O make this kind of analysis possible at least for these species.

3.1.1 The study region

PASE will be conducted east of Christmas Island (Kiritimati, 2 N, 157 W). This region was chosen because its chemistry and meteorology are well characterized and it is an ideal outdoor laboratory to study the chemistry of DMS. The chemical and aerosol characteristics have been reported by Bandy et al. [1996], Huebert et al., [1996], Clarke et al. [1996], Davis et al. [1999], and Chen et al. [2000]. The meteorological characteristics were reported by [Lenschow et al., 1999]. These investigations contain considerable detail so only the most relevant characteristics will be discussed here.

Christmas Island is in the southeast trade wind regime, far from anthropogenic sources of sulfur. Soundings of the 25 sps vertical velocity, water vapor mixing ratio, air temperature and ozone are shown in Figure 1. The

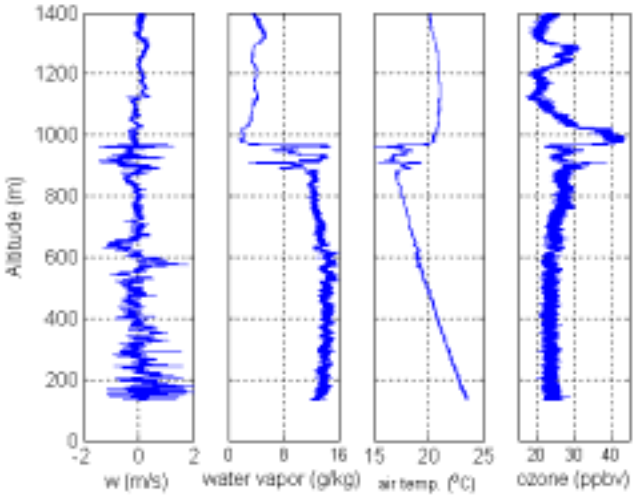

Figure 1 Soundings for vertical velocity, water vapor, air temperature and ozone in the Christmas Island trade wind system. The convective boundary layer (CBL) extends from the surface to about 630 m. The buffer layer (BuL) begins at 630 m and extends to about 970 m. The free troposphere is above 970 m.

CBL is characterized by a region of high and uniform fluctuations in vertical velocity that imply effective and rapid vertical mixing. Typical of turbulent layers, the sounding of water vapor is almost constant up to the CBL top where it rapidly decreases. The BuL is less well mixed because turbulence is weaker and intermittent. The top of the BuL is characterized by a further large drop in turbulence, water vapor, DMS, etc. at the trade wind inversion. Above the BuL is the free tropo-sphere.

An important property of the Christmas Island trade wind regime in August and September is that there are long periods during which few clouds exist especially in the CBL [Bandy et al., 1996]. The budget studies of PASE will be carried in one of these common, very stable, nearly cloud-free periods in August. However, aging, growth, and uptake onto aerosol will be enhanced in the small non-precipitating clouds that are often present in the BuL [Bandy et al., 1996]. Studies of cloud processing are an important component of PASE. Focus will be on both the nonprecipitating clouds that are often present in the BuL layer during the stable periods and the outflow of convective cumulus clouds that penetrate the trade wind inversion that often appear at the end of stable periods.

The characteristics of the CBL appear to be a general property of the marine trade wind regime. The soundings for DMS and vertical velocity in Figure 2 were obtained in the northeast trade wind regime in the Atlantic east of St. Croix, VI. Soundings for SO_2, vertical velocity and water vapor mixing ratio for Midway Island in the Pacific are shown in Figure 3. Each of these trade wind regimes has a turbulent, well mixed CBL and a less well mixed BuL.

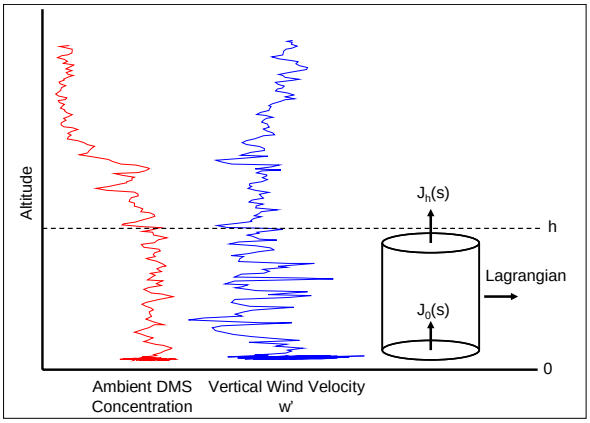

Figure 2 Soundings DMS and vertical velocity (1 Hz) for the trade wind regime east of St. Croix. The CBL depth is h and is about 800m.

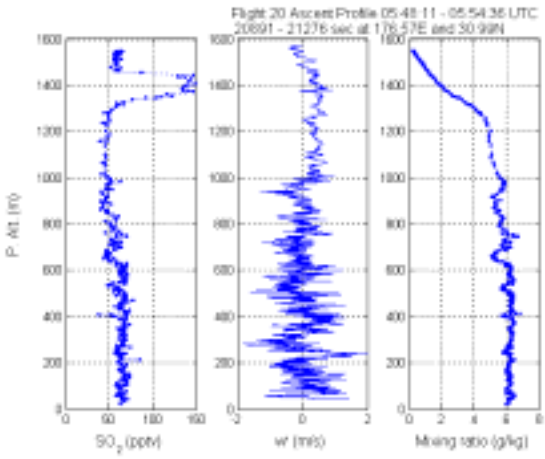

Figure 3 Vertical profiles for SO_2, vertical wind velocity and moisture mixing ratio for the Midway Island region. In this system the CBL extended to about 1 km with the buffer layer between 1 and 1.3 km. The SO_2 layer at about 1.4 km is in the free troposphere.

Because fluxes and time derivatives of concentrations are the variables to be measured in this study, requirements of homogeneity are greatly reduced (Lenschow, private communication) compared to previous studies of the Christmas Island trade wind regime [Bandy et al., 1996; Chen et al., 2000; Davis et al., 1999]. However, homogeneity makes data analysis easier and to some extent more precise.

East of Christmas Island for a few hundred kilometers, the ocean appears to have a reasonably homogeneous flux of DMS. Evidence of this homogeneity was obtained in Mission 7 of PEM Tropics A that was flown over a region 100 km in length just east of Christmas Island. In this mission level legs were flown as circles 60 km in diameter (30 minutes in length) that were advected with the mean wind. The variability of the concentrations along the track was small and very repeatable [Lenschow et al., 1999] and fit on a smooth curve determined by the photochemistry of the system [Davis et al., 1999]. To draw this inference of homogeneity it is useful to recognize that the CBL mixes vertically within the CBL in less than 0.5 hours (I. Faloona, private communication). Horizontal mixing is slower, so any change in surface flux quickly appears as a change in DMS around the circle. Systematic changes of this type were not observed at

Christmas Island [Lenschow et al., 1999]. Finally, Bandy et al. [1996] reported repeatable diel variations of DMS and SO_2 over 4 days that could not have been achieved unless the upstream DMS flux was reasonably uniform and constant.

3.1.2 Flight Plans

CBL budgets for DMS, SO_2, O_3, H_2O and possibly DMSO and $DMSO_2$ will be determined using the flight plan shown in Figure 4. Each set of legs will begin and end with a sounding to identify the top (h) of the CBL by locating the large decrease in variance of vertical velocity at the top of the CBL. Thirty-minute circles will then be flown at 30 m, h/2 and 3/4h and 4h/3 levels. This will be repeated 3 times. For nighttime missions the 30 m level can be flown only in daylight or twilight (for safety reasons). It is noteworthy that the soundings will be performed at 800 ft min^{-1} so the total expected duration for the sounding is about 3 min. The column concentrations of DMS, SO_2, DMSO, $DMSO_2$, and any other species with fast measurement rates will be obtained from these soundings. Since there will be 4 soundings per flight there will be 4 determinations of the column concentrations of these species, separated by about 2.5 hours. We will compute 3 time derivatives of the column concentrations of DMS, SO_2, DMSO, $DMSO_2$, and the other species with fast measurement rates. Finally short legs above the trade wind inversion will be flown at the beginning and end of the mission and possibly near the middle of the flight to characterize these regions. These will include soundings of the buffer layer.

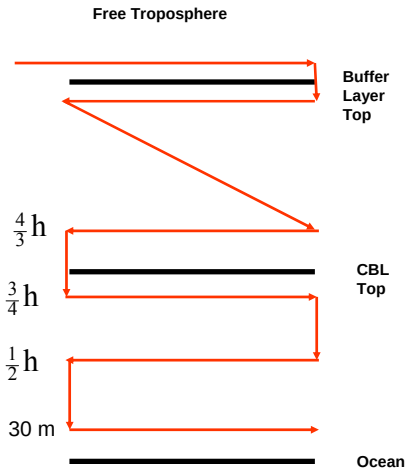

Figure 4 Flight profiles for CBL fluxes

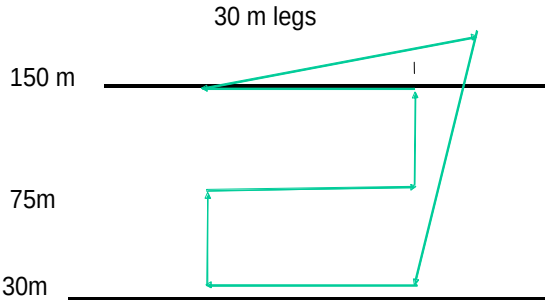

Figure 5 Flight profile for studying fluxes near the sea surface

Near-surface budgets of DMS and SO_2 and possibly of DMSO and $DMSO_2$ will be determined using the flight profiles shown in Figure 5. To minimize the impact of any variation in surface flux these studies will be flown over the same circle geographically to the extent possible, without entering the aircraft plume. These profiles will be flown 5 times per mission. Most of this flight will be flown under low light conditions to minimize photochemistry.

3.1.3 Meteorological Framework

As described in 3.1.1 the experiment will be carried out in the well mixed CBL east of Christmas Island. For this CBL the following budget approach provides the basis for interpreting data to be obtained in this study.

The budget for scalar s is given by the relationship

$$\frac{\partial \bar{s}}{\partial t} + \bar{u}\frac{\partial \bar{s}}{\partial x} + \frac{\partial \overline{s'w'}}{\partial z} = f(s) - d(s) \qquad (3.1.1)$$

The rate of change of each species is controlled by horizontal advection, vertical fluxes, formation, and destruction. Here s is the concentration of scalar s, $\bar{u}$ is the mean wind speed along the mean wind direction, x is the direction of the mean wind, w is the vertical velocity, z is the altitude, and $\overline{s'w'}$ is the eddy flux at

the altitude z. Also f(s) is the chemical formation rate and d(s) is the chemical destruction rate of s.

Integrating (3.1.1) from the surface through the top of the CBL yields

$$\frac{\partial \overline{< s >}}{\partial t} + \bar{u}\,\frac{\partial \overline{< s >}}{\partial x} - \bar{u}\,\Delta s\,\frac{\partial h}{\partial x} - J_0(s) + J_h(s) = F(s) - D(s) \qquad (3.1.2)$$

where angle brackets denote a column concentration for the boundary layer defined by

$$< s >= \int_0^h s\,dz \qquad (3.1.3)$$

Here h is the depth of the CBL, $J_o(s)$ is the flux at z=0, $J_h(s)$ is the flux at z=*h*, F(s) is the column chemical formation rate of s, and D(s) is the column chemical destruction rate of s. All missions will be flown in the Lagrangian framework (drifting patterns with the wind) so that $\bar{u}=0$. Equation (3.1.2) then simplifies to:

$$\frac{\partial < s >}{\partial t} - J_o(s) + J_h(s) = F(s) - D(s) \qquad (3.1.4)$$

All the terms on the left can be measured for DMS, H_2O, O_3 and SO_2. Budget analyses described below are based on (3.1.4).

3.1.4 How will equation (3.1.4) be used in this study?

The variable s represents the concentrations of O_3, SO_2, DMS, H_2O, or any other scalar quantity. Each of the terms has the units of flux, e.g., pptv m s^{-1} or molecules $m^{-2}s^{-1}$. As illustrated in Figure 2, (3.1.4) represents the conservation of mass of s in a cylinder that is moving at the mean wind speed along the direction of the mean wind. The chemical formation and destruction terms contain gas phase processes as well as gas-to-particle and particle-to-gas conversions. These issues are discussed in further detail in 3.5.

DMS data obtained during DYCOMS II illustrate the budget process. This program was a study of the dynamics of the stratocumulus regime west of San Diego that was conducted in the summer of 2001. The legs in the CBL were flown as 30 min circles, just as planned in PASE. Soundings for vertical wind velocity, liquid water, DMS and DMS flux are shown in Figure 6. (The stratocumulus region near San Diego is a one-layer system, so there is no BuL.) The CBLs of the stratocumulus and trade wind regimes are dynamically similar. Note the high uniform turbulence in the CBL as illustrated by the fluctuations in vertical velocity in the CBL and the transition to very low fluctuations at the top of the CBL. The almost constant DMS levels in the CBL reflect good vertical mixing. The flux of DMS increases with altitude in this case because dry, DMS-free air is being entrained at the CBL top and the DMS must be brought from lower altitudes to keep the DMS concentration constant with altitude. Note that the slope of the DMS flux vertical profile is the flux divergence of DMS.

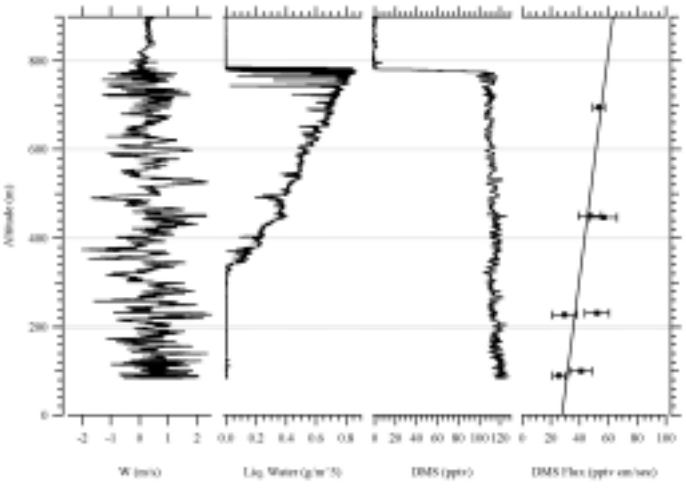

Figure 6 Soundings for vertical velocity, liquid water, DMS and DMS vertical flux. The slope of the DMS vertical flux curve is the vertical flux divergence of DMS.

Extrapolation of the DMS flux profile to the surface yields 27.5 pptv cm $s^{-1}$for the surface flux of DMS, J_0(DMS), and extrapolation to the CBL top yields 62 pptv cm s^{-1} for the flux for DMS at the CBL top, J_h(DMS). This is a general strategy for obtaining these two important quantities in the chemical budgets of the CBL. Computation of the time derivative of the column concentration of a scalar is straightforward and

is described in 3.2.1.

3.2 Strategy for computing real world chemical budgets

Because all terms on the left side of **(3.1.4)** will be experimentally determined, it is convenient to rewrite it in the form:

$$C(s)=F(s)-D(s) \tag{3.1.5}$$

where C(s) represents the difference between chemical formation and destruction, and can be experimentally determined:

$$C(s)=\frac{\partial < s >}{\partial t}-J_o(s)+J_h(s) \tag{3.1.6}$$

The program to determine complete CBL budgets will be designed so that one set of legs is flown at night. C(s) can be conveniently divided into nighttime processes that occur all the time and daytime processes that occur only during the daytime.

$$C(s)=F_n(s)-D_n(s)+F_g(s)-D_g(s) \tag{3.1.7}$$

$$C^{'}(s)=F_g(s)-D_g(s) \tag{3.1.8}$$

$$C_n(s)=F_n(s)-D_n(s) \tag{3.1.9}$$

$$C^{'}(s)=C(s)-C_n(s) \tag{3.1.10}$$

$F_g(s)$ and $D_g(s)$ are photochemical terms and are assumed to be gas phase processes as indicated by a g subscript. By flying one leg set at nighttime, $C_n(s)$ is obtained. Using standard propagation of errors techniques, the error in C(s) is obtained from the equation:

$$\delta C(s)=\sqrt{\left(\delta\frac{\partial <s>}{\partial t}\right)^2+[\delta J_o(s)]^2+[\delta J_h(s)]^2} \tag{3.1.11}$$

$$\delta C'(s)=\sqrt{[\delta C(s)]^2+[\delta C_n(s)]^2} \tag{3.1.12}$$

To estimate errors, $C_n(s)$ is assumed to be 10% of C(s). Therefore

$$\delta C'(s)=\sqrt{[\delta C(s)]^2+[0.1\delta C(s)]^2}\approx\delta C(s) \tag{3.1.13}$$

Although not as precise or complete there is another approach that requires only vertical profile data and does not require flux measurements. The full budget equation can be rearranged to yield

$$\frac{\partial < s >}{\partial t}=[J_o(s)-J_h(s)+F_n(s)-D_n(s)]+F_g(s)-D_g(s) \tag{3.1.14}$$

$$C'(s)=\frac{\partial < s >}{\partial t}-\left[\frac{\partial < s >}{\partial t}\right]_n=F_g(s)-D_g(s) \tag{3.1.15}$$

This approach assumes that the terms in square brackets in (3.1.14) do not change rapidly with time and is the preferred approach for a species that cannot be determined at 25 sps but can be determined at 1 sps or faster.

3.2.1 Propagation of errors in C(SO_2)

In this section the propagated errors in C(s) are computed for SO_2. The same strategy can be used to compute the propagated error in C(s) for DMS, DMSO and $DMSO_2$. Propagated errors for these species are summarized in Table 1.

From the soundings $<SO_2>$ can be computed at two different times, t_1 and t_2. From these data the time derivative of the SO_2 column concentration at each leg can be computed:

$$\frac{\partial \overline{< SO_2 >}}{\partial t}=\frac{< SO_2 >_2-< SO_2 >_1}{t_2-t_1} \tag{3.1.16}$$

The contribution of errors from instrumental noise is now computed for each sounding. At a data

rate of 25 sps, 4500 measurements of SO_2 are obtained in each 180 s sounding. With a conservative estimate of sensitivity of 60 counts per second per pptv and 60 pptv of ambient SO_2, a total of 648,000 counts are obtained in the 180 s interval. The standard deviation of this signal is the square root of the counts, which is 805. Here the error is estimated using the average of the SO_2 in the soundings. Note that this approximation is used only in making error estimates and not in the actual data processing.

The confidence interval for errors arising from detector noise is computed from the equation:

$$Confidence\ Interval(95\%) = \frac{t\sigma}{\sqrt{N}} = \frac{1.96 * 805}{\sqrt{4500}} = 24\ counts \tag{3.1.17}$$

Here t is the two tailed t value (1.96), σ is the standard deviation of the signal in counts (805 counts) and N is the number of measurements (4500). In pptv the confidence interval is

$$Confidence\ Interval\ in\ pptv(95\%) = \frac{24\ counts}{60\ counts\ pptv^{-1}} = 0.4\ pptv \tag{3.1.18}$$

Therefore

$$\delta\frac{\partial < SO_2 >}{\partial t} = h\left(\delta\frac{d[SO_2]}{dt}\right) = \frac{1000m * \sqrt{(0.4^2 + 0.4^2)\ pptv^2}}{7200\,s} = 0.08\,pptv\,ms^{-1} \tag{3.1.19}$$

Here the height of the boundary layer was assumed to be 1000 m and the error in the boundary layer height was negligible compared to other errors. Also the time between soundings is about 7200 s.

The error in the surface flux, $\delta J_o(SO_2)$, is computed using the fact that the eddy flux measurement technique can determine SO_2 fluxes to about 10% [Mitchell, 2001]. The surface flux of SO_2 on Christmas Island is estimated using the deposition velocity parameterization for J_0:

$$\left|J_o(SO_2)\right| = \upsilon_d[SO]_0 = 0.01\,ms^{-1} * 60\,pptv = 0.6\,pptv\,ms^{-1} \tag{3.1.20}$$

where v_d is the deposition velocity and $[SO_2]_0$ is the SO_2 concentration just above the ocean surface. The estimated error in the deposition velocity is 10% so the absolute error in $J_o(SO_2)$ is 0.06 pptv m s^{-1}.

The error in the flux at the CBL top would also be about 10% [Mitchell, 2001]. The entrainment velocity at the CBL top is about -0.005 m s^{-1}. The jump in SO_2 is assumed to be 60 pptv. The estimated flux at the boundary top is

$$\left|J_h(SO_2)\right| = w_e\Delta[SO]_h = 0.005\,ms^{-1} * 60\,pptv = 0.3\,pptv\,ms^{-1} \tag{3.1.21}$$

Since this flux also can be determined to 10%, the error is $\delta J_h(SO_2)$ = 0.03 pptv m s^{-1}. Assuming that $C_n(s)$ is 10% of C(s) the total error in C'(s) is 0.1 pptv m s^{-1}.

To put these errors into perspective, the formation rate of SO_2 is about 2 pptv m s^{-1} [Bandy et al. 1996; Mitchell 2001] so a 0.1 pptv m s^{-1} error in C'(SO_2) yields a relative propagated error of ≈5%.

Table 1. Estimates for uncertainty calculations

Molecule	v[1]	w[2]	h[3]	s[4]	J_0[5]	J_h[6]	δJ_0[7]	δJ_h[8]	<s>[9]	δ(d<s>/dt)[10]	δC'(s)[11]
SO_2	0.01	0.01	1000	60	0.60	0.30	0.06	0.03	60000	0.08	0.10
DMS	NA	0.01	1000	150	2.00	0.75	0.20	0.08	150000	0.12	0.25
DMSO	0.01	0.01	1000	20	0.20	0.10	0.02	0.01	20000	0.04	0.05
$DMSO_2$	0.01	0.01	1000.	20	0.20	0.10	0.02	0.01	20000	0.04	0.05

[1]Deposition velocity (ms^{-1})	[6] flux at CBL top (pptv m s^{-1})
[2] Entrainment velocity (ms^{-1})	[7]Error surface flux (pptv m s^{-1})
[3] CBL depth (m)	[8]Error in flux at CBL top (pptv m s^{-1})
[4] Concentration (pptv)	[9]Column concentration (pptv m^{-2})
[5] Surface flux (pptv m s^{-1})	[10]Error in time derivative of s (pptv m s^{-1})
	[11]Error in C'(s) (pptv m s^{-1})

3.2.2 *Daytime Studies*

The daytime studies must consider the fact that some species such as SO_2, DMSO and $DMSO_2$ can be destroyed by reaction with aerosol as well as photochemical processes. Loss to aerosol and photochemistry will be separately evaluated by flying a series of legs shown in Figure 4.

During daytime

$$C'(SO_2) = F_g(SO_2) - D_g(SO_2) \tag{3.1.22}$$

$$C'(DMS) = -D_g(DMS) \tag{3.1.23}$$

$$C'(DMSO) = F_g(DMSO) - D_g(DMSO) \tag{3.1.24}$$

$$C'(DMSO_2) = F_g(DMSO_2) - D_g(DMSO_2) \tag{3.1.25}$$

The gas phase formation rate of DMS is assumed to be negligible. The photochemical loss rate of SO_2 due to reaction with OH is slow and can be computed with small relative error. For example the reaction of OH and SO_2 has a rate constant of 1.5 x 10^{-12} $cm^3 molecule^{-1} s^{-1}$. The concentration of SO_2 is about 60 pptv or 1.47 x 10^9 molecules cm^{-3}, the daytime averaged OH is about 10^6 molecules cm^{-3} and the depth of the CBL is about 1000 m. Using these estimates $D(SO_2)$ from photochemistry is estimated to be 0.023 pptv m s^{-1}. Taking a conservative estimate of error of 30%, the contribution of this term to the overall error is 0.007 pptv m s^{-1} which is acceptable. For convenience this correction is included in $C'(SO_2)$. Therefore,

$$C'(SO_2) = F_g(SO_2) \tag{3.1.26}$$

The efficiency of conversion of DMS to SO_2 can be computed:

$$\%Eff = 100 \frac{|F_g(SO_2)|}{|D_g(DMS)|} \tag{3.1.27}$$

Here %Eff is the efficiency of conversion of DMS to SO_2 and ranges from 0 to 100%. To estimate an error in %Eff, the formation rate of SO_2 is assumed to be 1 pptv m s^{-1} and the destruction rate of DMS is assumed to be -2 pptv m s^{-1}. Using the data in Table 1 leads to a propagated error in %Eff of 15%. If the experiment is repeated 5 times the propagated error would be reduced to 7%.

The rate of reaction of OH and $DMSO_2$ is probably negligible compared to other processes such as the loss to aerosol [Davis et al., 1998], so the gas phase chemical column destruction rate of $DMSO_2$, $D_g(DMSO_2)$, is negligible. Consequently, $F_g(DMSO_2)$ is uniquely determined:

$$C'(DMSO_2) = F_g(DMSO_2) \tag{3.1.28}$$

The fraction of DMS leading to DMSO can be approximated by that which is not converted to SO_2:

$$F_g(DMSO) = |D_g(DMS)| \left(1 - \frac{\%Eff(SO_2)}{100}\right) \tag{3.1.29}$$

In this way the destruction rate of DMSO can be determined as a function of time. Also the efficiency of the formation of $DMSO_2$ from DMSO can be estimated

$$\%Eff = 100 \frac{|F_g(DMSO_2)|}{|D_g(DMSO)|} \tag{3.1.30}$$

Nighttime circles are flown in the same way as the daytime circles except that the 30 m leg must be flown in twilight for safety reasons.

3.2.3 *Full Nighttime Budgets.*

At night we assume (for now) that the chemical formation rates of most s are negligible. Hence

$$C(s) = -D(s) \tag{3.1.31}$$

D(s) is probably negligible for DMS but not necessarily for the other species where it contains a contribution from loss to aerosol. However, in this case D(s) will be small because most of the sea salt aerosol

removing s is located below the lowest leg flown. In this case most of the loss of s to aerosol is included in $J_0(s)$. A separate experiment to study this issue is described in 3.2.4.

3.2.4 Studies of s just above the ocean surface

Just above the ocean surface a layer of basic sea salt particles having large surface area is thought to remove s. Several missions will be flown to provide quantitative determination of the removal of s by aerosol. This study will be focused on the region below 150 m where a large fraction of the loss of s to aerosol is expected [Suhre et al., 1995]. In this study 3 circles will be flown at 30, 75, and 150 m. Three flight levels were chosen because the reactivity of s in this region may change with height producing nonlinear changes in $J_0(s)$ with height within this layer. The choice of three levels was a compromise between available time on station and the need to account for this nonlinear behavior. The 30 and 75 m circles will be flown during twilight for safety reasons.

The relative contribution of loss of s to the sea surface and loss of s to aerosol can be estimated. The budget equation for s in integral form for this region from the surface to 150 m is

$$C(s) = -D(s) \tag{3.1.32}$$

$J_0(s)$ is the true surface flux that will be obtained by fitting the fluxes at 30, 75, and 150 m to a quadratic and then extrapolating J(s) to the surface to obtain $J_0(s)$. The percentage loss of s to aerosol below 150 m compared to the total loss in the region being studied including that lost at the ocean surface is given by the expression:

$$\%\,Lost\ Aerosol < 200m = \frac{|D(s)|}{|D(s)| + |J_o(s)|} \times 100 \tag{3.1.33}$$

This can be done only for any species that can be determined at 25 sps and will include both DMS and SO_2.

To compute an estimated error in the loss of s to aerosol we assume that the rate of loss of s to aerosol is equal to the rate of loss of s to ocean surface. For SO_2 the propagated error in the *% lost to aerosol* is 16%. **.** This error can be decreased by repeating this experiment 5 times under conditions of similar wind speeds in which case the error would be reduced to 7%.

The many additional measurements in PASE allow a more detailed study of the boundary layer budget of sulfur to be performed near the ocean surface. For instance, the aerosol surface area will be measured, allowing an estimate of the loss rate of SO_2 to aerosol to be compared with the result from the gas phase analysis described in this section. The observed deficit of Cl and Br in various sizes of aerosol can be combined with an estimate of the flux of sea salt aerosol to estimate the source of gas phase halogens from the sea salt aerosol. This will be compared to the rate at which SO_2 is lost to aerosol.

3.2.5 Dependence of $J_0(s)$ on wind speed

In the summer of 1994 the Christmas Island meteorology occurred in regimes in which the atmosphere was near steady state for 3-4 days in which the wind speed gradually increased from 5 to 10 m s^{-1}. During days 6 and 7 the wind speed increased gradually to about 12 m s^{-1}. This kind of variability provides an opportunity to investigate the surface fluxes of s and the losses of s to aerosol during a more than doubling of the wind speed. Models indicate a significant change in SO_2 surface flux and loss to aerosol as the wind speed increases. Some models suggest the magnitude of exchange velocities for gas emission increase with the cube of the wind speed [Wanninkhof and McGillis, 1999]. Computation of exchange velocity requires the surface ocean concentration measurements. However, the concentration of SO_2 in the surface ocean is negligible, thus the exchange velocity of SO_2 can be determined by extrapolating vertical fluxes made at higher altitudes to the ocean surface. The wind speed dependencies of the DMS, SO_2, H_2O and O_3 surface fluxes will be compared.

3.2.6 Nighttime budget of DMS

At nighttime both the chemical formation and destruction rates of DMS should be negligible. Therefore

$$F(DMS) = D(DMS) = 0 \quad (3.1.34)$$

As described above C(DMS) can be determined to about 0.25 pptv m s^{-1}. Since the chemical formation of DMS in the atmosphere is assumed to be negligible the magnitude of the chemical destruction rate of DMS and the formation rate of SO_2 during nighttime can be shown to be ≤0.25 pptv m s^{-1}. Although the destruction rate of DMS and the formation rate of SO_2 should be zero at night, this experiment allows us to test the assumption that halogen and nitrate radical reactions are unimportant at night in this region.

3.3 Eddy Fluxes and entrainment velocities

Ian Faloona (UC-Davis), supported by a Drexel contract, is responsible for the field assessment of the fast data obtained in PASE. This includes DMS, SO_2, H_2O, and O_3, and some meteorological parameters. He and Don Lenschow will be responsible for the computation and interpretation of eddy fluxes and the computation and interpretation of budgets (along with the Drexel group). Faloona also is responsible for the determinations of the entrainment velocities and work with other groups in their application to budgets of species not determined with sufficient speed to apply eddy correlation.

The entrainment velocity is defined by the relationship

$$\left[\overline{s'w'}\right]_h = -w_e \Delta s \quad (3.1.35)$$

Here $\left[\overline{s'w'}\right]_h$ is the eddy flux at the CBL top obtained by extrapolating eddy fluxes obtained at various altitudes in the CBL to the CBL top. Also w_e is the entrainment velocity and Δs is the jump in s at the CBL top. In the DYCOMS II program DMS flux data were used to obtain good estimates of the entrainment velocity [Faloona et al., 2005; Stevens, 2003]. Estimates of the entrainment velocities will be obtained from DMS, H_2O, SO_2, O_3, momentum, and heat during PASE.

4 Investigators

Dr. Alan Bandy is the mission scientist and is responsible for the execution of the field program and organizing the interpretation and publication of the data. Dr. Byron Blomquist (U. Hawaii) will be responsible for the fast SO_2, DMS, DMSO and $DMSO_2$ measurements. OH, H_2SO_4, MSA and NH_3 will be determined by Dr. Lee Mauldin (NCAR). Dr. Jim Hudson (Desert Research Institute) will make CCN measurements. Dr. Anthony Clarke will perform aerosol size, thermal properties and composition measurements. Drs. Barry Huebert and Steve Howell (U. Hawaii) will make aerosol composition measurements. Drs. Brian Heikes, John Merrill (U. Rhode Island) and Dr. Daniel O'Sullivan (US Naval Academy) will provide H_2O_2 and CH_3OOH data and meteorological support. Drs. Ian Faloona (UC-Davis) and Donald Lenschow (NCAR) will direct mission planning and the aircraft mission as well as assisting in the eddy correlation analyses. Drs. Yuhang Wang and Douglas Davis (Georgia Tech) will provide photochemical modeling.

5 Measurements

Byron Blomquist (U. of Hawaii) has the overall responsibility for the sulfur gas measurements under contract to Drexel University. He will operate the DMS instrument and will oversee the efforts of two Drexel University personnel (one undergraduate and one postdoctoral associate), who will operate the SO_2 and DMSO/$DMSO_2$ instruments. Alan Bandy will also help provide in flight supervision when not involved with his mission scientist duties.

5.1 Measurement of SO_2

The determination of SO_2 will be determined at 25 sps. SO_2 is determined using the following reactions [Mohler et al., 1992]; [Thornton et al., 2002]:

$$O_3^- + CO_2 \rightarrow O_2 + CO_3^- \quad (4.1.1)$$

$$SO_2 + CO_3^- \rightarrow SO_3^- + CO_2 \quad (4.1.2)$$

$$SO_3^- + O_2 + M \rightarrow SO_5^- + M \quad (4.1.3)$$

The SO_2 concentration is proportional to the SO_5^- that is monitored at 112 amu. $^{34}S^{16}O_2$ is added to the manifold continuously as an internal standard and is determined as SO_5^- at 114 amu. Because the sensitivity of the instrument can be continuously computed from the $^{34}S^{16}O_2$ signal and the instrument is known to be linear, the only other parameter needed to compute the SO_2 concentration is the blank. The blank can be determined using a scrubber consisting of a short length of copper tubing. Using isotope dilution in the RICO program this method of establishing a zero for SO_2 was shown to be very efficient. It quantitatively and quickly removes SO_2 from air in the marine environment [D.C. Thornton, private communication].

5.2 Determination of DMS

DMS is determined using the following reactions [*Bandy et al.*, 2002]:

$$N_4^+ + H_2O \rightarrow H_2O^+ + 2N_2 \quad (4.1.4)$$

$$H_2O + H_2O^+ \rightarrow H_3O^+ + OH \quad (4.1.5)$$

$$H_3O^+ + nH_2O + N_2 \rightarrow H_3O^+(H_2O)_n + N_2 \quad (4.1.6)$$

$$H_3O^+(H_2O)_n + DMS \rightarrow DMSH^+(H_2O)_m + (n+1-m)H_2O \quad (4.1.7)$$

$$DMSH^+(H_2O)_m + M \rightarrow DMSH^+ + mH_2O + M \quad (4.1.8)$$

Ambient DMS is proportional to the $DMSH^+$ signal at 63 amu. Reactions 4.1.7 and 4.1.8 are equilbria, which at high water vapor concentrations typical of the marine boundary layer favor the water clusters of $DMSH^+$ [*Sunner et al.*, 1988a; *Sunner et al.*, 1988b; *Xu*, 1999]. This clustering can be reduced to negligible values by predrying the air and heating it to a high temperature in the ionizer. This approach was highly successful for DMS whose sensitivity was very dependent on moisture levels. The DMS sensitivity was completely restored by predrying and heating [*Bandy et al.*, 2002].

DMS-d_3 is added to the manifold continuously as an internal standard and is monitored at 66 amu. Because the sensitivity of the instrument can be continuously computed from the $DMSH^+$-d_3 signal and the instrument is known to be linear, the only other parameter needed to compute the DMS concentration is the blank [*Bandy et al.*, 1993; *Bandy et al.*, 1992; *Bandy et al.*, 2002]. DMS was successfully determined at 25 sps during the DYCOMS II program [Faloona et al., 2005].

5.3 Determinations of DMSO and $DMSO_2$

DMSO and $DMSO_2$ will be determined using methods that are virtually identical to the determinations of DMS by APIMS has been described in the previous section [*Bandy et al.*, 2002], although they have not been presented in the journal literature. However, they are described in detail in Xu's PH.D. dissertation [*Xu*, 1999] and are similar to those used by Nowak et al [2001].

5.4 OH, HO_2, H_2SO_4, MSA and NH_3

Measurements of OH, HO_2, H_2SO_4, MSA and NH_3 will be determined by Dr. Lee Mauldin (NCAR). Support of the determinations of OH, H_2SO_4, MSA and NH_3 and other selected radicals by Dr. Lee Mauldin (NCAR) is included here as a subcontract. The above compounds will be measured using a multi-channel selected ion chemical ionization mass spectrometer (SICIMS) (Davis et al.,1999; Nowak et al., 2002; Cantrell et al., 2003), which is an improved version of the instrument used previously aboard the NCAR C-130 for the NSF-sponsored TOPSE study. With the exception of ammonia, these compounds have all been successfully measured on a near simultaneous basis in several previous airborne studies. Measurements of OH, H_2SO_4, and MSA will be on a time shared basis every 30 sec, resulting in a detection limit of 0.1 pptv (parts per trillion by volume) in 1 minute and 0.02 pptv in 5 minutes respectively for each species. Peroxy-radicals will be measured on an exploratory basis using a second separate mass spectrometer channel. Either HO_2 or HO_2+RO_2 will be measured once every 30 sec, with a 0.1 pptv detection limit for a 1 min. integration. NH_3 will be measured using a third mass-spectrometer channel once every 15 sec with a detection limit of ~30 pptv for a 2 minute integration.

5.5 CCN

CCN spectra will be determined by Dr. James Hudson (Desert Research Institute) and is supported here by a subcontract to Drexel University. The two DRI CCN instruments obtain spectra simultaneously and continuously from droplet spectral size distributions from their cloud chambers (Hudson, 1989). Both of these instruments have been mounted on the NCAR C-130 for six different projects—MSCT (1994), SCMS (1995), SHEBA (1998), INDOEX (1999), AIRS2 (2003), and RICO (2004-2005). A calibration curve converts measured droplet sizes (128 channels of pulse voltages) to particle critical supersaturation (S_c), which is calculated based on size and composition as verified by Gerber et al. (1977). The calibration particles are obtained by DMA size classification of polydisperse aerosol of known composition (e.g., NaCl). It is assumed that droplet growth within the cloud chambers is directly related to the S_c of each particle regardless of size or composition because S_c accounts for both. Since S_c should always represent the response of particles to applied supersaturation, then particles with the same S_c should produce the same droplet sizes in the cloud chamber.

There is speculation that this principle may not hold for all particle compositions when organic films may be involved (Shulman et al. 1996; Facchini et al. 1999; Feingold and Chuang 2002). However, extensive agreement between these two instruments that has so far been obtained argues against this possibility (Hudson and Da, 1996; Hudson and Yum, 2002). Moreover, the clean maritime air to be encountered in PASE is the most unlikely place to find such deviations from the original Kohler theory (Mircea et al., 2000).

The two DRI instruments obtain complete CCN spectra simultaneously and continuously in two overlapping ranges extending from supersaturations (S) of 0.01% to 3% and the capability to obtain spectra at rates as fast as 1 second. This is well below the 0.1% lower limit of other CCN instruments. This is important because roughly half of CCN have $S_c < 0.1\%$. The characterization of these largest particles is vital for static CCN closure - comparisons of particle size and composition with CCN concentrations, which is an important goal of PASE. Periodic volatility measurements (Hudson and Da, 1996; Hudson and Yum, 2002) can easily distinguish NaCl.

5.6 Aerosols

Aerosol measurements will be made by Drs. Clarke, Howell, and Huebert (U. of Hawaii). Each of these investigators has submitted their own detailed proposals so only a summary is included here.

Because the products of those gas-phase reactions are often aerosols, a large suite of aerosol physical and chemical measurements will be made. Continuous fast size-resolved measurements of ambient aerosol surface area will be determined to estimate rates of loss of gaseous sulfur species to aerosol (Clarke). These measurements will include ambient size-distributions, dry size distributions and both wet and dry scattering coefficients that can be used to confirm both size distribution measurements. Continuous measurements of thermally resolved dry aerosol size distributions will be used to estimate the 3-D changes in aerosol size due to both nucleation and uptake of volatile components (Clarke). These size-resolved measurements will address issues related to the contributions of entrainment and DMS derived sulfates to aerosol variability. It will also provide evaluation of the role of refractory sea-salt aerosol, its flux, and its contributions to aerosol volume, surface area and number.

The aerosol chemical measurements will be used to measure the bulk chemical composition of ionic constituents. This will include cations sodium, ammonium, potassium, magnesium, calcium, and anions chloride, nitrate, sulfate, and methane sulfonate in small particles [up to 1 micrometer]. Aerosol chemistry will also be collected using the Total Aerosol Sampler (TAS), which collects even the largest sea salt particles without inlet bias (Huebert) and analyzed for cations and anions (Howell). The other methods may miss the coarse fraction of NSS, which results from the ozone oxidation of SO_2 in sea salt. A MSP Flying MOUDI (MOI) with a low-turbulence inlet (LTI) on the aircraft will be used to get size-resolved chemistry from the aircraft (Howell). Because many of the mission legs will be flown as 30 minute level legs, integrated samples taken over a complete leg will provide high precision concentration data for these aerosol substances.

6 Flight Plans

In July or August 2007 the C-130 will be ferried from RAF to Christmas Island. Some portions of this ferry can be used for research. However, this is not the primary goal of the mission.

The field phase of the program will be conducted about 250 km east of Christmas Island (Kiritimati). Approximately 5 weeks onsite will be devoted to this study so that the best available meteorological conditions can be chosen for study. As mentioned above the stable meteorological phases tend to be 3-4 days in length with the overall length of a stable-unstable period being approximately 7 days. In 5 weeks approximately 4 stable periods are expected which provides ample opportunities to complete this research. The plan presented below assumes that the flights will be flown at every opportunity that does not exceed crew rest requirements. There may other adjustments if critical measurement systems are not operational.

Table 2 Flights for Budget Studies

Flight	Time	Duration	Purpose
1	Night*	9	Nighttime budgets
2	Night*	9	Surface Fluxes
3	Night*	9	Nighttime budgets
4	Day	9	Daytime Budgets
5	Day	9	Daytime Budgets
6	Day	9	Daytime Budgets
7	Day	9	Daytime Budgets
8	Night*	9	Nighttime budgets
9	Night*	9	Surface Fluxes
10	Night*	9	Surface Fluxes

*Nighttime flights will conform to NCAR RAF safety

In addition to these budget study flights, three 9 hours missions will be flown to investigate the formation of nuclei in the outflow of cloud and BuL processes described in previous sections. These flights will be flown when conditions are favorable. Satellite and meteorological support is described briefly in a previous section and in detail in the Heikes and Merrill proposal.

6.1 Field activities

Alan Bandy will serve as overall mission scientist of the field phase. Most important he will be the interface between the RAF and the PASE scientists. He is responsible for all decisions concerning science in the mission. He will organize mission planning, select flight dates and mission, and will be make decisions on safety issues not covered by RAF. He will be present in the cabin on all flights to work with PI's to make sure all remain informed on flight progress and important issues. He will aid the PI's in obtaining access to the aircraft for instrumentation repair and testing during non flight days. Ian Faloona will fly in the cockpit and will be the interface between the pilots and Alan Bandy on all flight issues. Faloona also will monitor the progress of the flight as well as some important instruments.

Between missions Bandy will debrief each of the PI's to establish the progress of their measurements. He will work with Merrill to establish the current meteorology and then present this information to scientists at a planning meeting held one day before flights.

Merrill has the responsibility of providing relevant meteorological data. Stable meteorological phases should be easily recognized. The beginning of such a phase is characterized by very steady winds at speeds of 4-6 m $s^{-1}$and a direction of almost 100^{o}. Also the skies are almost cloud free (cloud free in CBL) with very bright sunshine. Decision to fly can be made the previous evening with good prospects for the flight program the next day. A detailed discussion of using satellite and other meteorological information to guide aircraft deployment is included in the Merrill proposal (University of Rhode Island).

6.2 Data Processing and Dissemination

It is the responsibility of the mission scientist to archive all the data produced by this experiment. Workshops to discuss the data and plan publications will be held 6, 12, and 18 months after the completion of the experiment. The data archive will enter the public domain through a web site at NCAR 1.5 years after completion of the experiment. It is the intent to publish a special volume in an appropriate journal.

6.3 Other Activities

PASE will have a substantial instructional component both at the undergraduate, graduate, and post-

doctoral level. A Drexel University undergraduate student and the post doc will each operate one of the instruments for determining SO_2, DMSO and $DMSO_2$ on the C-130 and will have the responsibility of processing and reporting the data to the PASE archive. Under the supervision of Byron Blomquist and Alan Bandy, the students and the post doc will interpret and publish papers based on their data. The graduate student will focus on the PASE data for a thesis dissertation. One female undergraduate student is currently working in the Bandy research group. In the past year a second undergraduate student from the Drexel Honors program participated in data analyses for the RICO program as an REU. This student also has expressed an interest in continuing this association with the Bandy research group. Additional Drexel students will be given the opportunity to participate in PASE data interpretation through our Chemistry research courses (Chemistry 493 and 497), which are required of all chemistry majors.

Several undergraduate students, graduate students and post docs from Georgia Tech, the University of Hawaii and the University of Rhode Island will be involved in both the field and interpretation phase of the program. These activities are described in the proposals of individual PI's. Each PI has agreed to present a seminar to students during the field campaign at Christmas Island. PI's will also be encouraged to request that students attend workshops and make presentations when appropriate.

A website will be developed to communicate the progress of the field mission including Google Earth with aircraft flight tracks and data. This application is in development at RAF for the HIAPER and we hope to apply this approach for PASE. We will publicize the site through cooperative links to The Academy of Natural Sciences and The Franklin Institute in Philadelphia as well as The Philadelphia Inquirer.

7 ATD/RAF Airborne Scientific Instrumentation requested

The following RAF instruments will be requested in addition to the standard airborne scientific measurements supplied by RAF: Lyman-alpha hygrometer, Gerber probe (liquid water content), cloud particle size distribution (0.5 - 47 μm), cloud particle size distribution (40 - 640 μm), aerosol particle size distribution (0.1 - 3.0 μm), aerosol particle size distribution (0.3 - 20 μm), fast-response chemiluminescence ozone concentration, video recording (fwd) with optional date/time stamp, video recording (side) with optional date/time stamp, video recording (down) with optional date/time, audio recording (on video tape) stamp, 1 sec digital photos should be available in at least the forward direction.

8 Results from Prior NSF Support

OPP-9809162, Investigation of the sulfur chemistry of the Antarctic troposphere (ISCAT), $391,813, 5/14/98 - 12/31/02

SO_2, DMS, DMSO, $DMSO_2$ and MSIA (methane sulfonic acid) were determined at the South Pole during November and December of 1999 using Atmospheric Pressure Ionization Mass Spectrometry. These data and those of participating principal investigators were processed and archived. SO_2 was the predominant sulfur gas other than carbonyl sulfide. After 18 Dec 2000 the meteorological conditions changed, and the concentration of the sulfur gases (other than carbonyl sulfide) were <5 pptv. Sulfur dioxide was frequently observed at the clean air station from aircraft and local sources (primarily vehicles).

D. D. Davis, F. Eisele, G. Chen, J. Crawford, G. Huey, D. Tanner, D. Slusher, L. Mauldin, S. Oncley, D. Lenschow, S. Semmer, R. Shetter, B. Lefer, R. Arimoto, A. Hogan, P. Grube, M. Lazzara, A. Bandy, D. Thornton, H. Berresheim, H. Bingemer, M. Hutterli, J. McConnell, R. Bales, J. Dibb, M. Buhr, J. Park, P. McMurry, A. Swanson, S. Meinardi and D. Blake, An overview of ISCAT 2000, Atmos. Environ.., 38, 5363-5373, 2004.

ATM-0002655, An Airborne Study of the Chemistry of Sulfur in the Atmosphere of the Western North Pacific Ocean, 7/1/2000-6/30/2002, $329,220

Sulfur dioxide was determined on ACE-ASIA with a frequency of 2 Hz and a lower limit of detection of 3 pptv. The data were processed and submitted in the ACE Asia archive (CODIAC, JOSS, UCAR). The SO_2 data clearly showed transport was predominantly at altitudes below 2000 m above sea level.

M. Chin, P. Ginoux, R. Lucchesi, B. Huebert, R. Weber, T. Anderson, S.J. Masonis, B. Blomquist, A.R. Bandy, D. Thornton, A global aerosol model forecast for the ACE-Asia field experiment, J. Geophys. Res., 108, D23, 8654, doi:10.1029/2002JD3642, 2003.

C.S. McNaughton, A.D. Clarke, S.G. Howell, K.G. Moore, V. Brekhovskikh, R.J. Weber, D.A. Orsini, D.S. Covert, G. Buzorius, F.J. Brechtel, G.R. Carmichael, Y.H. Tang, F.L. Eisele, R.L. Mauldin, A.R. Bandy, D.C. Thornton, B. Blomquist, Spatial distribution and size evolution of particles in Asian outflow: Significance of primary and secondary aerosols during ACE-Asia and TRACE-P, J. Geophys. Res., 109, D19S06, doi:10.1029/2003JD003528, 2004.

T. Murayama, S. J. Masonis, J. Redemann T. L. Anderson, B. Schmid, J. M. Livingston, P. B. Russell, B. J. Huebert, S. G. Howell, C. S. McNaughton, A. Clarke, M. Abo, A. Shimizu, N. Sugimoto, M. Yabuki, H. Kuze, S. Fukagawa, K. Maxwell-Meier, R. J. Weber, D. A. Orsini, B. Blomquist, A. Bandy, D. Thornton, An intercomparison of lidar-derived aerosol optical properties with airborne measurements near Tokyo during ACE-Asia, J. Geophys. Res., 108, 8651, doi:10.1029/2002JD3259, 2003.

ATM-0004444, A Study of the Dynamics of the Marine Stratocumulus, 2/1/2001- 1/31/2003, $190,396
Dimethyl sulfide was determined with a frequency of 25 Hz. The data were processed and archived with the DYCOMS II data in CODIAC (JOSS, UCAR). DMS was used to determine the entrainment velocity at the stratocumulus cloud top. The entrainment velocity determinations from DMS, ozone, and thermodynamic properties agreed within experimental limits. DMS surface fluxes were also obtained.

B. Stevens, D. H. Lenschow, I. Faloona, C-H. Moeng, D. K. Lilly, B. Blomquist, G. Vali, A. Bandy, T. Campos, H. Gerber, S. Haimov, B. Morley, D. Thornton, On Entrainment Rates in Nocturnal Marine Stratocumulus, Quart. J. Roy. Meteorol. Soc., 129, 3469-3493, 2003.

B. Stevens, D. H. Lenschow, I. Faloona, C-H. Moeng, D. K. Lilly, B. Blomquist, G. Vali, A. Bandy, T. Campos, H. Gerber, S. Haimov, B. Morley, D. Thornton, Dynamics and Chemistry of Marine Stratocumulus - DYCOMS-II, Bull. Amer. Meteor. Soc., 84 (5), 579-593, 2003.

I. Faloona, D. Lenschow, T. Campos, B. Stevens, M. van Zanten, B. Blomquist, D. Thornton, Alan Bandy, Observations of Entrainment in Eastern Pacific Marine Stratocumulus Using Three Conserved Scalars, J. Atmos. Sci., 62, doi: 10.1175/JAS3541.1, 3268–3285, 2005.

ATM-342672, Chemistry of Sulfur Dioxide and Dimethyl Sulfide in the Tropical Marine Boundary Layer, 2/1/2004-7/31/2005, $248,594
Work is in progress testing atmospheric pressure ionization mass spectrometry techniques for dimethyl sulfoxide and dimethyl sulfone. Field tests for DMSO indicated possibility to obtain <1 Hz time resolution for DMSO and $DMSO_2$.

ATM-0342138, High Rate Determinations of Dimethyl Sulfide and Sulfur Dioxide during Rain In Cumulus over the Ocean (RICO), 3/1/2004-2/28/2006, $289,262
Field phase of RICO was conducted in December 2004 and January 2005. Data reduction and analyses are in progress. An undergraduate student was involved in the data analyses for the summer of 2005.

ATM-0421920, Development of a Method for Gaseous Hydrogen Peroxide Using Airborne Atmospheric Pressure Ionization Mass Spectrometry, 8/1/2004-7/31/2006, $135,351
Work is in progress testing atmospheric pressure ionization mass spectrometry techniques for hydrogen peroxide. An undergraduate student was involved in the research for the summer of 2005.